中國機械工程學刊第四十卷第五期第 515~522 頁(民國一百零八年)
Journal of the Chinese Society of Mechanical Engineers, Vol.40, No.5, pp 515~522 (2019)

Tolerance Design of Low Noise Humidifier using Monte Carlo and Multi-body Dynamic Simulation

Jungwoo Lee*, Junhyuck Jang**, Jaehoon Sim* and Weuibong Jeong ***

Keywords： tolerance design, Monte Carlo simulation, multi-body dynamic simulation, spur gear.

ABSTRACT

In case of general home appliance product, resin parts are widely used due to economic efficiency and structural design freedom. However, Resin parts have shape and dimensional variations depending on the injection and cooling conditions when they are injected. When various parts are assembled, the accumulated tolerances may cause degradation of product performance or NVH problem. Particularly, the tolerance of the system in which its operating conditions are varied during operation becomes greater. In this study, Monte Carlo simulation is used to obtain the tolerance variation of the humidifier parts considering the changing operating conditions. And multibody dynamics analysis is also used to secure the operability of the driving part and low noise level. Experiments were also carried out to verify the noise and vibration level. This study is expected to be useful in the early stage of research before prototyping.

INTRODUCTION

Tolerance Design

Many studies have been conducted in the field of robust design, tolerance design, and optimum design considering reliability in order to deal with the uncertainty that necessarily exists in the engineering system. In these design methods, statistical analyses are generally used to estimate the distribution of the quality characteristics and reliability.

As simple methods, there are worst case analysis and root-sum-square(RSS) analysis. For complex system analysis, Monte Carlo simulation, reliability index method or de-sign of experiment method can be used. Since the worst-case analysis uses the upper and lower limits of the tolerance, it is not suitable for general product design because it causes excessive design. The RSS method uses the linear equation of Taylor series on the assumption that the nominal value and the mean value are same, so that the excessive design problem is alleviated, but there is a limit to the nonlinear system. The reliability index method requires the calculation of the derivative of the system's first or second order approximate expression in the iterative process to obtain reliability, so when the non-normal distribution is included, many errors occur in the process of approximating the normal distribution. D'Errico and Zaino (1988) have applied the three level experimental design method proposed by Taguchi and the Gauss quadrature method to reduce the computational load of the computer. However, the computational processing speed and capacity of computers has rapidly developed, allowing complex products including nonlinear problems to be quickly analyzed through Monte Carlo simulations. C. Kim (2015) proposed a tolerance design method corresponding to thermal deformation using Monte Carlo analysis and FEM.

Target System and Research Objectives

Figure 1 is a vertical section and a photo of the home appliance with air purifying, deodorizing and humidifying functions. The air passing through the air cleaning and deodorizing filter module (a) is humidified while passing through the humidifying wheel (b) absorbed from the humidifying water reservoir (c) and discharged to the room through the air blowing fan (d). Here, the structure in the dotted line is a drawer type filter module, which can be pulled to open the front of the product for water resupply and maintenance. When the drawer is closed, the gear on the humidifying wheel (b) and the driving gear (e) are

Paper Received April, 2019. Revised September, 2019. Accepted October, 2019, Author for Correspondence: Jungwoo Lee

* *Chief Research Engineer, LG Electronics, Korea*

** *Senior Research Engineer, LG Electronics, Korea*

*** *Professor, School of Mechanical Engineering, Pusan National University, Korea*

engaged to rotate the humidifying wheel. The absorbed water is diffused throughout the rotating wheel with the speed of 0.5 RPM.

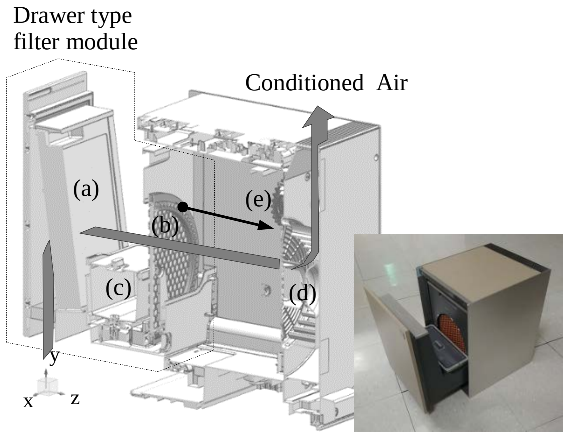

Fig.1. Vertical section view and a photo of the bedroom humidifier.
(a) Air filter
(b) Humidifying wheel with driven gear
(c) Water supplier (d) Blowing fan
(e) Driving gear

The most parts of this product are made of resin such as ABS, polypropylene and polystyrene. And, since this product is design for a bedroom, it is necessary to have low noise performance that does not disturb when the user sleeps.

The objectives of this study are to predict the locational variation of gears by assembly tolerance using Monte Carlo simulation and then to accomplish the following objectives using multibody simulation.

1. The power transmission of gears should be ensured despite assembly tolerances.
2. Even if the drawer closes with minimal force, the gears should be engaged gently without collision between the gears.
3. Noise should be at a level that does not interfere with sleep at a distance of 50 cm from the product.

50 cm is the distance between the product and the user head when the product is placed next to the bed.

VARIATION PREDICTION OF HUMIDIFYING WHEEL

Identification of Distribution Form

An exploratory data analysis is required prior to statistical study, as statistical quantities of data may be distorted if there are biases or outliers. Some physical quantities such as stress or surface roughness are naturally biased. In non-normal distribution cases, statistical analysis can be performed by correcting to the normal distribution by the Box-cox transformation method depending on the distribution form.

In the short term, the variation of shapes or sizes of injection resin parts occurs due to the difference in cooling rate depending on the anisotropy and thickness of the material. And in the long term, it is caused by a change of injection condition due to seasonal change. Therefore, in order to design the tolerance of the assembly structure of the injection molding parts, variations of at least one year must be considered.

The manufacturer manages the allowable tolerance. Table 1 shows the general management levels of the injection molding parts.

Table 2 and Figure 2 show the results of analyzing the data of the incoming inspection for the past two years. Seven parts have been selected by size from similar products in production and data were obtained. Since the measurement data are obtained by using digital vernier calipers at the incoming inspection, the measurement error of the measurer is included in addition to the actual error.

Table 1. Tolerance control limit according to injection molding parts size.

Class / Range, mm	J	K	L	M	N	Angle JKL	Angle MN
R ≤ 10	0.05	0.2	0.3	0.5	0.7	1°	6°
10 < R ≤ 30	0.1	0.3	0.5	0.8	1.2		
30 < R ≤ 50	0.2	0.4	0.6	1.1	2.0	30’	2°
50 < R ≤ 150	0.3	0.6	0.8	1.4	2.5		
150 < R ≤ 300	0.4	0.8	1.0	1.7	3.5	15’	1°
300 < R ≤ 500	0.6	1.2	1.5	2.0	4.5		
500 < R	0.8	1.6	2.0	2.5	5	5’	30’

Table 2. Statistics of size variations of injection molding parts.

SD: standard deviation

Nominal, mm	12.8	36.2	53.5	83.5	180.2	316.0	585.5
Tolerance, mm	±0.3	±0.3	±0.3	±0.6	±0.6	±0.6	±0.6
Data N	72	64	56	69	84	58	88
Mean, mm	12.8	36.2	53.5	83.6	180.4	315.9	585.4
Min., mm	12.7	36.0	53.2	83.3	180.0	315.7	585.0
Max., mm	12.9	36.3	53.8	83.8	180.7	316.2	585.8
SD, mm	0.06	0.08	0.11	0.11	0.15	0.12	0.17
P-value	0.70	0.97	0.83	0.42	0.51	0.51	0.71

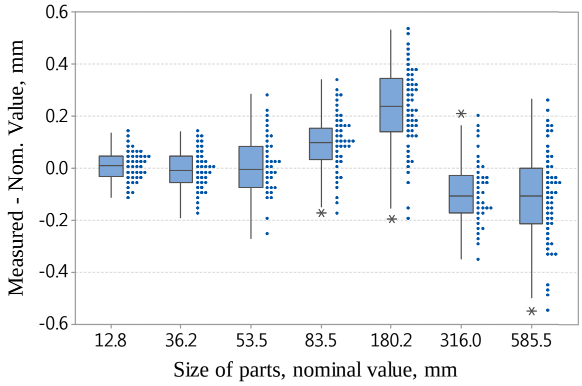

Fig.2. Box and dot plot of size distribution of injection molding parts.

The dimensional variation due to cooling and flow during injection is affected by the thickness and length of the parts, so that the standard deviation in the Figure 2 tends to increase as the size of the component increases.

In the Table 2, the P-value is the result of testing the normality by the Anderson-Darling method. This result shows that the variation of the resin parts can be expressed as a normal distribution. However the average values out of zero in the Figure 2 are not the problems of tolerance design. It may be offset caused by wear of the mold or variations in the injection environment.

Relational Expression to Determine the Location of the Humidifying Wheel Center

In order to obtain the locational variation of humidifying wheel center according to the dimensional variation of other parts, the product is schematically shown in Figure 3.

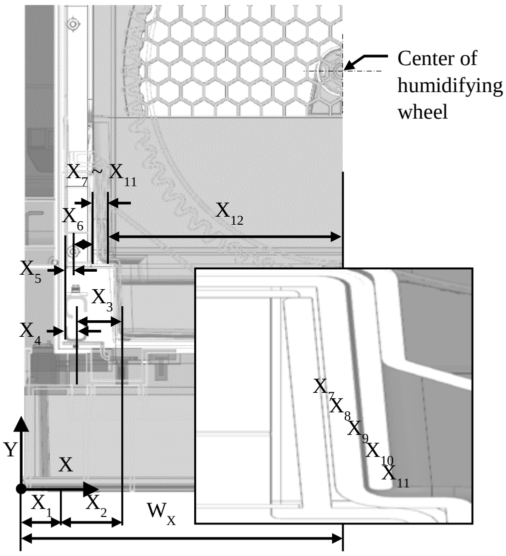

(a) Schematic for determining the center of humidifying wheel, X-axis

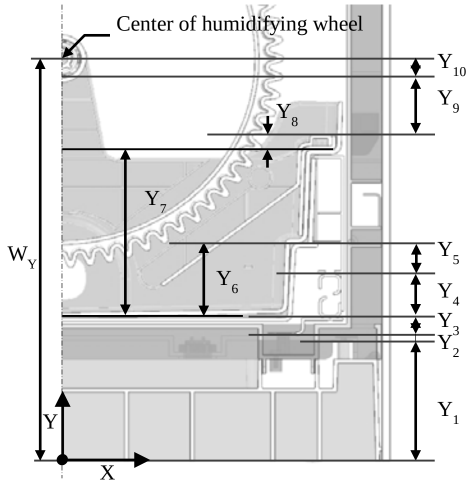

(b) Schematic for determining the center of humidifying wheel, Y-axis

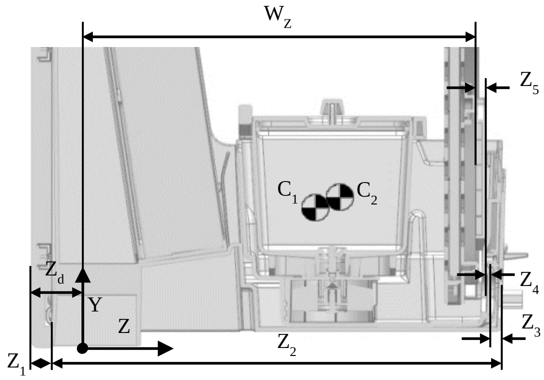

(c) Schematic for determining the center of humidifying wheel, Z-axis
C1: Mass center of empty water tank
C2: Mass center of water tank is full with 3 liter of water

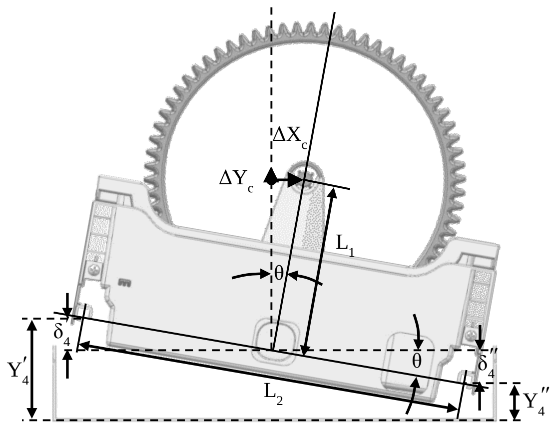

(d) Change of center of humidifying wheel due to tilting of drawer

Fig.3. Schematics for determining the center of humidifying wheel

The drawer is constrained by a pair of 310 mm slides with ball bearing arranged in the Z direction. So the variation by the yawing motion which is the Y axis rotation can be ignored. In addition, as shown in Figure 3 (c), the center of gravity of the filter module is biased and tilted toward the humidifying wheel. So the variation by the pitching motion, which is the X axis rotation of the filter module, is represented by variation in the Y direction.

The relations of determining the center position *W* of the humidifying wheel can be obtained as follows by using the diagram of Figure 3 (a), (b) and (c).

$$W_X = X_1+X_2-X_3-X_4+X_5+X_6 +X_7+X_8+X_9+X_{10}+X_{11}+X_{12} \quad (1)$$

$$W_Y = Y_1+Y_2+Y_3+Y_4+Y_5-Y_6+Y_7+Y_8+Y_9+Y_{10} \quad (2)$$

$$W_Z = Z_1+Z_2-Z_3-Z_4-Z_5-Z_d \quad (3)$$

In equation (3), Z_d is the gap of the door that occurs when the drawer door is closed. As in Figure 3 (d), rolling motion of the filter module, which is the Z axis rotation, occurs as shown by variation of a pair of Y axis positions Y_4' and Y_4'' on both sides of the ball bearing slide. Here, the locational change of the humidifying wheel center caused by rolling is as follows.

$$\Delta X_c = L_1 \times \sin\theta \quad (4)$$

$$\Delta Y_c = L_2 \times (\cos\theta - 1) \quad (5)$$

Where,

$$\theta = \sin^{-1}((\delta_4' - \delta_4'')/L_2) \quad (6)$$

$$\delta_4' = Y_4' - \widehat{Y}_4, \qquad \delta_4'' = Y_4'' - \widehat{Y}_4 \quad (7)$$

$\widehat{Y}_4$ is the nominal value of Y_4' and Y_4'', and is substituted in equation (2) as follows.

$$\widehat{Y}_4 = (Y_4'+Y_4'')/2 \quad (8)$$

Consideration of Environmental Variables and Minimize Impacts

When the reservoir with 3 liter capacity at Figure 1 (c) is fully filled with water, the 3.0 kg load of water causes deformation of the lower part of the drawer. As a result of deformation, the locational variation of the humidifying wheel center is expected.

Figure 4 shows the result of analysis of the maximum deformation caused by water of 3.0 kg using the structural analysis FEM tool ANSYS.

The amount of change in the X and Y directions of the humidifying wheel center (a) is negligible as 0.00 and -0.03 mm, respectively, but a maximum -0.92 mm change occurs in the Z axis. This change is mainly due to the lack of strength of supporter (b). So, as shown in Figure 5, the strength of the supporter was reinforced by the rib design to reduce the deformation amount to -0.52 mm, which is 56%.

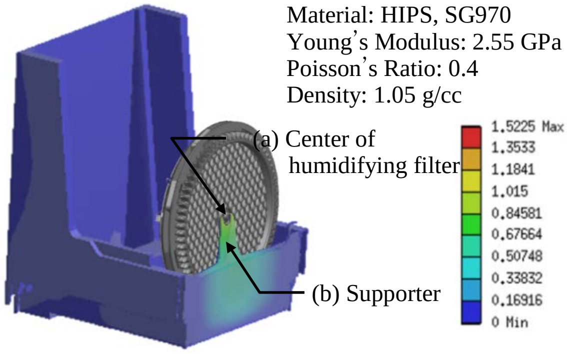

Fig.4. Deformation analysis result by FEM tool, ANSYS

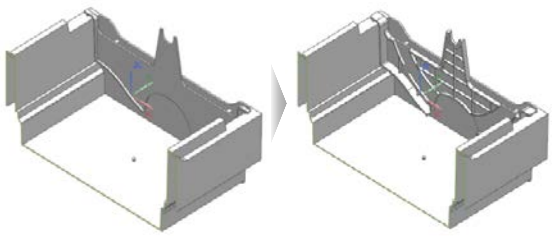

Fig.5. Structural reinforcement with ribs to reduce deformation

The effect of reducing the variation by improving the stiffness of the supporter is shown in Figure 7.

The locational change in the Z axis of humidifying wheel center is denoted by ΔZ_c

Variation Prediction of Humidifying Wheel Center Position using Monte-Carlo Simulation

Since the Monte Carlo simulation is recommended to perform more than 100,000 times, a corresponded random number is generated for each variable.

Unlike most data in normal distribution, the distribution of the door closing Z_d has a distribution with long tail to the right. Weibull, log normal or chi-square distribution can be used in a distribution with a Y axis intercept of 0 and a right long tail. Among them, Weibull distribution is widely used for reliability analysis because of its high degree of freedom of shape. Based on the data of existing similar products, we generated 100,000 random data by Weibull distribution with shape parameter 2, scale parameter 0.4, and zero point parameter 0, as shown in Figure 6 using Minitab 17.

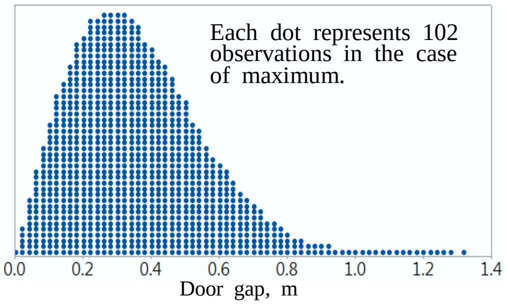

Fig.6. Simulated distribution of door gap with Weibull distribution

In the case of ΔZ_c, the change of the humidifying wheel center by the water, is in the recoverable linear deformation range and the water weight is the uncontrollable variable as an environmental condition, so the uniform distribution random data is generated in the range of 0 and -0.52mm.

When the rolling motion of the drawer filter module and the deformation by water are applied to the equations (1), (2) and (3), they are as follows.

$$W_X = X_1+X_2-X_3-X_4+X_5+X_6 +X_7+X_8+X_9+X_{10}+X_{11}+X_{12}+\Delta X_c \quad (9)$$

$$W_Y = Y_1+Y_2+Y_3+Y_4+Y_5-Y_6+Y_7+Y_8+Y_9+Y_{10}+\Delta Y_c \quad (10)$$

$$W_Z = Z_1+Z_2-Z_3-Z_4-Z_5+Z_d+\Delta Z_c \quad (11)$$

The average value of the random data generated for each variable is their nominal value, and the standard deviation is derived from the linear regression of the Table 2 data.

In this way, the variation of the humidifying wheel center is simulated with 100,000 data sets, and the dispersion in the three-dimensional space is shown in Figure 7.

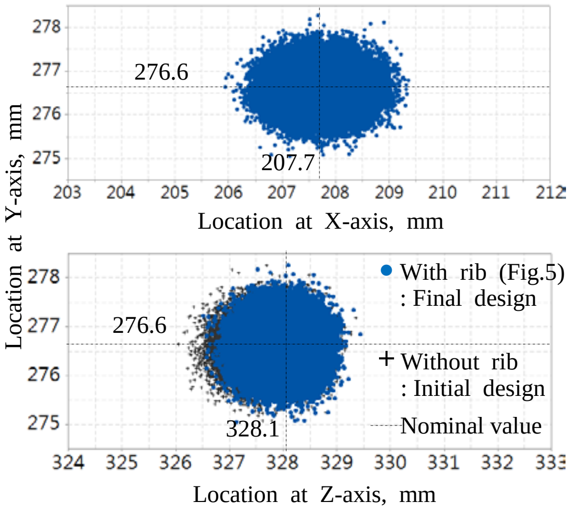

Fig.7. Monte Carlo simulation for center of humidifying wheel

DESIGN OF GEARS

Design for Axial Direction Coupling

For axial coupling and power transmission, a face gear and a spur gear were considered as shown in Figure 8.

The drawer structure design is applied to this product, so there is little space for arranging parts in the Z direction. In case of a face gear, the driving gear was limited to a maximum outside diameter of 34 mm and a whole depth of 4.3 mm. As shown in Figure 7, when the tolerance in the Z direction is 2.7 mm, it lost 63% of the working depth and the power transmission was impossible. And a face gear has another problem that structure-born noise is amplified when negative tolerance. For these reason, a spur gear has been selected for this system.

In order to prevent interference between the gears when the drawer is closed, the taper is applied on the gear teeth in the axial direction. And circular boss is also applied on the driving gear teeth to induce gear engagement gently by point contact of the boss. Then, the face width of the gear shown in Figure 8 (d) is designed to be 6.0 mm so as to have a safety factor of 2.2 with a Z axis variation of 2.7 mm, shown in Figure 7.

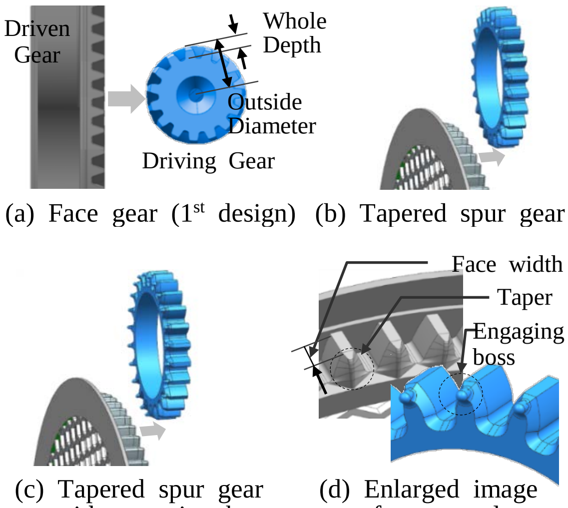

(a) Face gear (1st design) (b) Tapered spur gear

(c) Tapered spur gear with engaging boss (final design) (d) Enlarged image of taper and engaging boss

Fig.8 Gear design for axial direction coupling and operability

Figure 9 shows the result of simulating the needed force to be engaged according to the relative position of the gears when the gear contacts in the axial move. Three types of gear sets, face gear, spur gear without boss and spur gear with engaging boss are shown. As a magnet is applied at the drawer, so that even if the user closes drawer with minimum force, it can be closed gently, and the force of magnet generated at that time is 5 N. In the case of spur gears with an engaging boss, the needed force is less than 5

N at all relative gear positions, which indicates that the gears can be engaged in any case.

On the other hand, in the case of a spur gear without a boss, a needed force of 20 N occurs near 0 degrees at which the contact between the gears occurs. In the case of face gear, 45 N is needed at maximum because it is impossible to apply taper at the gear teeth.

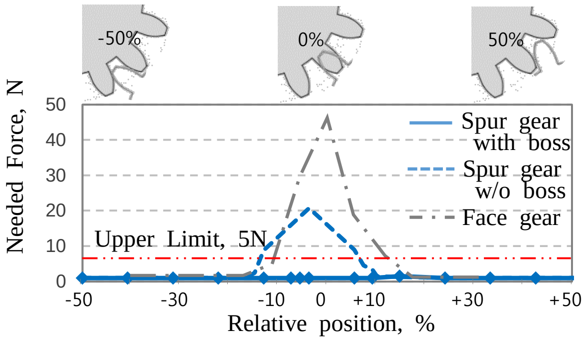

Fig.9 Needed force to engage gears according to relative gear position

Design for Operability on X-Y Plane

The multi body dynamics analysis tool RecurDyn is used to analyze the operable range according to the relative positions of the gears in the X-Y plane, and the results obtained by overlaying the scatter plot of the humidifying wheel center of Figure 7 are shown in Figure 10.

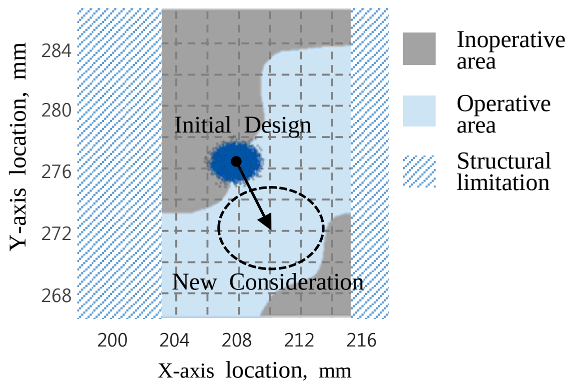

Fig.10 Multi body simulation result of operability according to gear position

In the case of the initial design where the design nominal value of the humidification wheel center is X: 207.7, Y: 276.6 mm, the power transmission may fail depending on the assembly tolerance situation, so moving to the new consideration area is considered.

LOW NOISE DESIGN

Simulation of Real Time Torque Variation of Gears

Figure 11 shows the multi body dynamic simulation results of the torque fluctuation when the position between the gears is changed by the assembly tolerance for the face gear and the spur gear corresponding to Figure 8 (a) and (c). In each case is simulated with the maximum tolerance condition. Since the rotational speed of the humidifying wheel is 0.5 RPM, it is analyzed for 2 seconds corresponding to 1 cycle.

Face gears are vulnerable to changes in relative position between gears, while spur gears are robust to assembly tolerances. This result is not an inherent characteristic of a face gears but rather a result of the face gear having a small diameter and a small number of teeth. Due to the structure of the product, there is a restriction in the Z direction, so that the design restriction of the spur gear is freer than the face gear in this system.

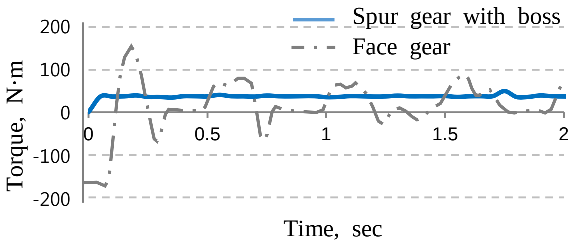

Fig.11 Multi body simulation result of torque fluctuation
: Gear offset ΔX: -1.7, ΔY: -0.5, ΔZ: -1.6 mm

The average noise is proportional to the average of the generated torque, and when the variation of the torque becomes large, it leads to the fluctuation of the real time noise (2006). That is, it is possible to minimize the noise by designing the generated torque and the variation to be minimal.

Of course, the passive noise countermeasures such as resonance avoidance design of the structure, shielding of aerodynamic noise and reduction of structural noise transmission are also discussed separately.

Figure 12 shows the torque average and standard deviation for one cycle in the previously selected spur gear and the newly selected design region.

The X and Y axes were analyzed at intervals of 0.5 mm. According to previous studies about low noise product, the torque average is within 110% of the lowest level and the torque standard deviation is within 130% of the lowest level. The white region of Figure 12 corresponds to torque average of 4.17 N·m (110% of the minimum 3.79 N·m) and torque standard deviation of 0.08 N·m (130% of the minimum 0.06 N·m).

Therefore, the nominal value of the humidifying filter center coordinate is changed to X 208.7, Y 271.5 mm.

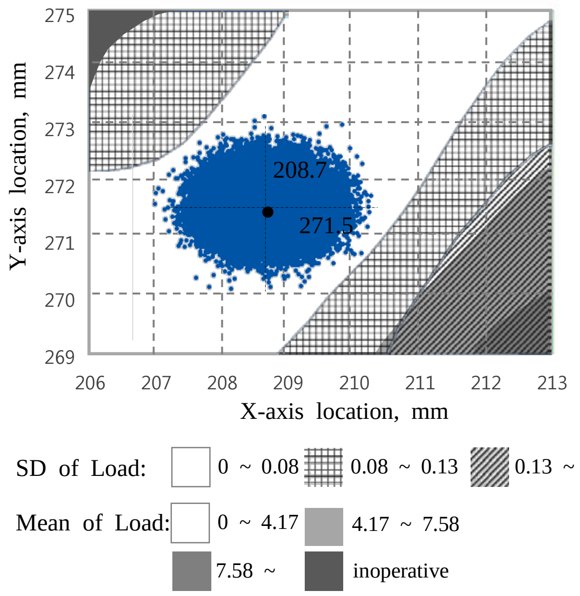

Fig.12 Multi body simulation result of torque mean and standard deviation

EXPERIMENTAL TEST

Noise Level Measurement

Since product concept is a bedside table, when the noise is measured, a wall is installed on the back side of the product as shown in Figure 13, and the microphones are placed at 50cm distance. LMS SCADAS was used as the measuring instrument, and GRAS 1/2 free field microphones were used as the microphone.

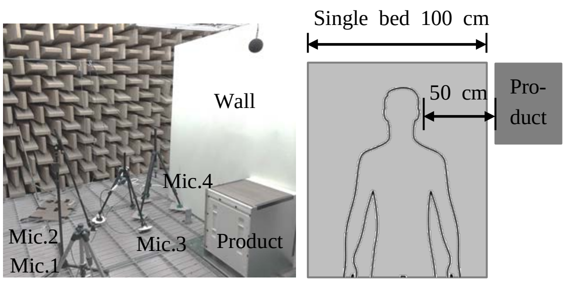

Fig. 13 Experimental setup for measuring noise level

As a result of the above study, it was possible to reduce the noise from the initial noise level of 23.4 to 20.8 dBA, and the abnormal noise caused by the gear friction was removed. The real-time noise waterfall spectrum of the initial and improved design are shown in Figure 14.

The product noise was reduced to 19.0 dBA through further improvement of the fan and the motor mount design. These contents are not included in this paper.

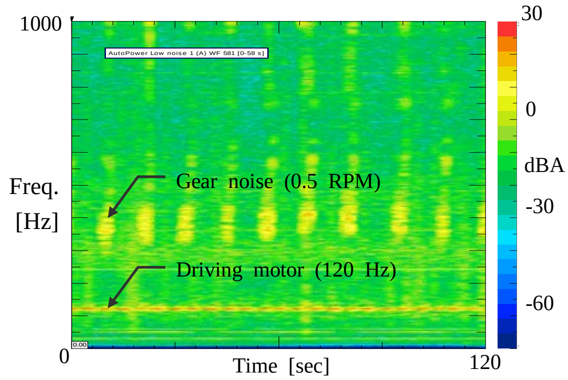

(a) Initial design: Overall noise level 23.4 dBA

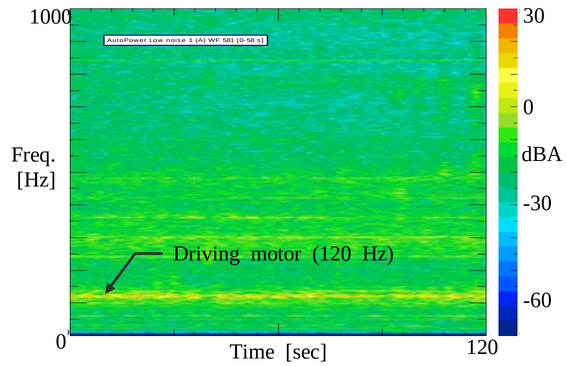

(b) Modified : Overall noise level 20.8 dBA

Fig. 14 Noise level measurement experimental setup and result

According to ANSI standard S12.2-2008, noise level of low noise operation mode has been measured with TÜV Rheinland, an international product testing and certifying company and the result is shown in Figure 15. (Report # 50110448 001) The product noise level shows that it satisfies the NC-20 rating, which corresponds to the recording studio.

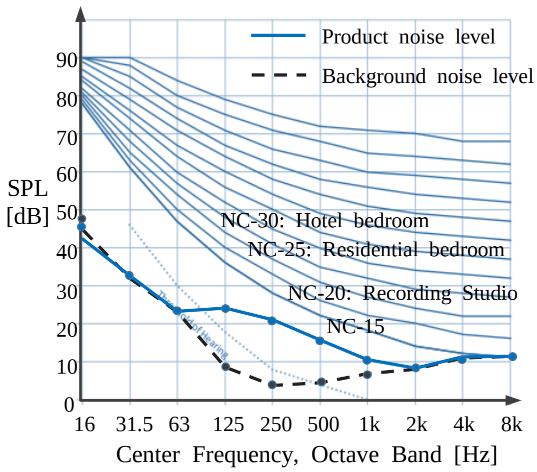

Fig. 15 Noise measurement result with octave band

Operability and Gear Engagement Performance Test

During the product development stage, 10 products were manufactured and tested for 3,600 times of drawer opening / closing tests corresponding to 10 years use. The number of operation and gear engagement failure was zero.

CONCLUSIONS

In this paper, we have proposed a design method of driving part that can operate robustly against assembly tolerance by using Monte-Carlo simulation and multi body dynamic simulation. In particular, by plotting the mean and the standard deviation map of the drive torque obtained by multi body dynamic analysis together with the assembly variation, it is possible to maintain low noise performance. Experiments were also conducted to verify the usefulness of this technique.

The general research process that can be applied to these topics is summarized as follows.

1) Identification of variation patterns and modeling of environmental variables
2) Understanding mechanism of accumulated tolerance by creating schematic diagram of interest part or system
3) Structural improvement to reduce tolerances
4) Design of driving part to deal with tolerance
5) Low noise design through the average and variance maps of drive torque
6) Experimental verification

REFERENCES

Cheulgon Kim and Jihoon Hwang, “Study of the Assembly of Indoor Air-conditioner Unit Using Tolerance Analysis , *Korean Soc. Mech. Eng.*, Vol. 39, No. 4, 423-428 (2015).

D.R.House, Gear Noise and Vibration Prediction and Control Methods, John Wiley & Sons (2007).

J.D. Smith, Gear noise and vibration, Marcel Dekker (2003).

Jinsu Kim and Jaesung Kim, “Tolerance Analysis and Design of Refrigerator Door System for Functional and Aesthetic Quality of Gap and Flush”, *J. Korean Soc. Precis. Eng.*, Vol. 31, No. 1, pp. 59-66 (2014).

John R. D'Errico and Nicholas A. Zaino, Jr., “Statistical Tolerancing Using a Modification of Taguchi's Method”, *Technometrics*, Vol. 30, No. 4, pp.397-405 (1988).

K. Krishnamoorthy, Handbook of Statistical Distributions with Applications, Chapman and Hall/CRC (2006).

Santiago Velilla, “A Note on the Multivariate Box-Cox Transformation to Normality”, *University of Madrid, Working Paper*, pp. 92-08 (1992).

Yu. A. Shreider, The Monte-Carlo Method: The Method of Statistical Trials, Elsevier (1966).

NOMENCLATURE

SD standard deviation

C center of gravity

X_n, Y_n, Z_n nominal value of corresponding dimension

Z_d dimension of drawer gap in Z axis

$\Delta X, \Delta Y, \Delta Z$ change of humidifying filter center

δ change of locational coordinate

L length

θ rotation angle

基於 Monte Carlo 和多體動力學模擬的低雜訊加濕器公差設計

李晶雨 張俊赫 沁在勳 鄭義峰

LG 電子空調研究實驗室

摘 要

在普通家用電器產品的情況下，由於經濟效率和結構設計自由度，塑膠部件被廣泛使用。然而，塑膠部件的形狀和尺寸變化取決於注射時的注射和冷卻條件。當組裝各種部件時，累積 的公差可能導致產品性能下降或 NVH 問題。特別是，在操作期間其操作條件變化的系統的公差變得更大。在本研究中，考慮到操作條件的變化，使用 Monte Carlo 模擬來獲得加濕器部件的公差變化。並且多體動力學分析還用於確保驅動部件的可操作性和低雜訊水準。還進行了實驗以驗證雜訊和振動水準。預計該研究在原型製作之前的研究早期階段是有用的。